

## Oxidizing Ru(II) Complexes as Irreversible and Specific Photo-Cross-Linking Agents of Oligonucleotide Duplexes

Liana Ghizdavu,<sup>†</sup> Frédéric Pierard,<sup>†</sup> Stéphane Rickling,<sup>†</sup> Sabrina Aury,<sup>†</sup> Mathieu Surin,<sup>‡</sup> David Beljonne,<sup>‡</sup> Roberto Lazzaroni,<sup>‡</sup> Pierre Murat,<sup>§</sup> Eric Defrancq,<sup>§</sup> Cécile Moucheron,<sup>†</sup> and Andrée Kirsch-De Mesmaeker<sup>\*†</sup>

<sup>†</sup>Université libre de Bruxelles, Chimie Organique et Photochimie CP 160/08, av. F.D. Roosevelt 50, B-1050 Brussels, Belgium, <sup>‡</sup>Service de Chimie des Matériaux Nouveaux, Université de Mons, 20, Place du Parc B-7000 Mons, Belgium, and <sup>§</sup>Département de Chimie Moléculaire, UMR CNRS 5250, Université Joseph Fourier BP 53, 38041 Grenoble Cedex 9, France

Received May 25, 2009

Oxidizing polyazaaromatic Ru<sup>II</sup> complexes containing two TAP ligands (TAP=1,4,5,8-tetraazaphenanthrene) are able under illumination to cross-link irreversibly the two strands of an oligonucleotide (ODN) duplex by covalent bond formation. The cross-linking proceeds by two successive absorptions of a photon. An adduct of the metallic complex on a guanine (G) base of one ODN strand is first photoproduct, followed by a second photoaddition of the same Ru species to a G base of the complementary strand, provided that the two G moieties are separated by 0 or 1 base pair. These two processes lead to the cross-linking of the two strands. Such a photo-cross-linking is easily detected with [Ru(TAP)<sub>2</sub>(phen)]<sup>2+</sup> (**1**; phen=1,10-phenanthroline) and [Ru(HAT)<sub>2</sub>(phen)]<sup>2+</sup> (**2**; HAT=1,4,5,8,9,12-hexaazatriphenylene), whereas it is not observed with [Ru(TAP)<sub>2</sub>TPAC]<sup>2+</sup> (**3**; TPAC = tetrapyridoacridine) at the same level of loading of the duplex by **3**. With a concentration of **3** similar to that of **1** and **2**, when the loading of the duplex by **3** is much more important than with **1** and **2**, the photo-cross-linking with **3** can thus also be observed. As **3** intercalates its TPAC ligand into the base pairs stack, its mobility is restricted in the duplex. In contrast, **1** and **2** can adopt different geometries of interaction, which probably facilitate the photo-cross-linking.

### Introduction

The mononuclear Ru<sup>II</sup> complexes that contain at least two  $\pi$ -deficient polyazaaromatic ligands such as TAP (TAP = 1,4,5,8-tetraazaphenanthrene) or HAT (HAT = 1,4,5,8,9,12-hexaazatriphenylene; Figure 1) are known to behave as oxidizing agents under illumination, capable of extracting one electron from guanine bases (G) in mononucleotides, polynucleotides, and DNA.<sup>1</sup> This photoelectron transfer (ET) studied for one TAP complex with DNA by laser flash photolysis in the picosecond time domain, was suggested to be coupled to a proton transfer.<sup>2</sup> The pair of radicals formed after this ET gives rise either to the back ET or to the formation of a photoproduct. The latter corresponds to a covalent adduct of the complex on the guanine base, the structure of which is shown in Figure 2 for TAP and HAT

complexes with a guanine (G) base or guanosine-5'-monophosphate (GMP).<sup>3,4</sup>

Within the scope of the use of antisense oligonucleotides for gene silencing applications, we have developed a strategy to photo-cross-link the two complementary strands of an oligodeoxyribonucleotide (ODN) duplex on the basis of this photoreaction. Thus, a photoreactive oxidizing Ru<sup>II</sup> complex comprising two TAP ligands is chemically tethered to one ODN strand (the probe sequence), which after hybridization with its complementary strand (the target sequence) and subsequent visible illumination produces a photoadduct of the attached complex to a guanine base of the complementary target strand. This reaction occurs provided the target strand contains a G base in the vicinity of the attached complex. As a result, the two strands are cross-linked,<sup>5</sup> a process that

\*To whom correspondence should be addressed. E-mail: akirsch@ulb.ac.be.

(1) Herman, L.; Ghosh, S.; Defrancq, E.; Kirsch-De Mesmaeker, A. *J. Phys. Org. Chem.* 2008, 21, 670–681 and references therein.

(2) Elias, B.; Creely, C.; Doorley, G. W.; Feeney, M. M.; Moucheron, C.; Kirsch-De Mesmaeker, A.; Dyer, J.; Grills, D. C.; George, M. W.; Matousek, P.; Parker, A. W.; Towrie, M.; Kelly, J. M. *Chem. Eur. J.* 2008, 14, 369–375.

(3) Jacquet, L.; Davies, R. J.; Kirsch-De Mesmaeker, A.; Kelly, J. M. *J. Am. Chem. Soc.* 1997, 119, 11763–11768.

(4) Blasius, R.; Nierengarten, H.; Luhmer, M.; Constant, J.-F.; Defrancq, E.; Dumy, P.; van Dorsselaer, A.; Moucheron, C.; Kirsch-De Mesmaeker, A. *Chem. Eur. J.* 2005, 11, 1507–1517.

(5) (a) Elias, B.; Kirsch-De Mesmaeker, A. *Coord. Chem. Rev.* 2006, 250, 1627–1641 and references cited therein. (b) Deroo, S.; Le Gac, S.; Ghosh, S.; Villien, M.; Gerbaux, P.; Defrancq, E.; Moucheron, C.; Dumy, P.; Kirsch-De Mesmaeker, A. *Eur. J. Inorg. Chem.* 2009, 524–532.

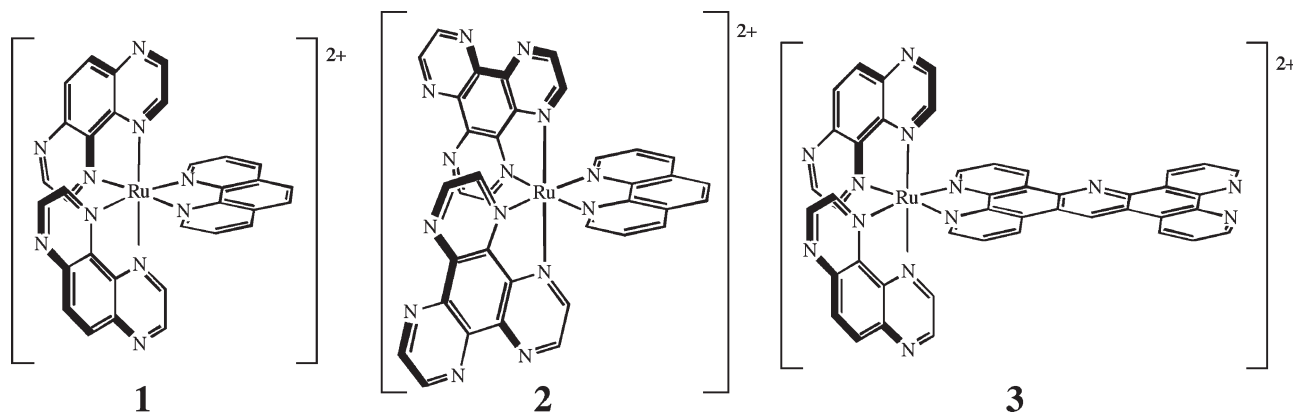


**Figure 1.** Structure of  $[\text{Ru}(\text{TAP})_2(\text{phen})]^{2+}$  (1),  $[\text{Ru}(\text{HAT})_2(\text{phen})]^{2+}$  (2), and  $[\text{Ru}(\text{TAP})_2\text{TPAC}]^{2+}$  (3).

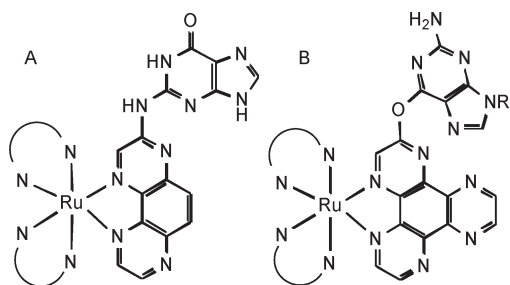


**Figure 2.** Structures of the photoadducts of the Ru complexes at the level of (A) a TAP ligand with a G base and (B) a HAT ligand with a guanosine monophosphate ( $\text{R} = \text{phosphoribose}$ ).

damages DNA and inhibits the exonuclease activity with 100% efficiency.<sup>6</sup>

Although very interesting for gene silencing, such Ru-ODN probes suffer from a drawback, which is the derivatization of the ODN by the photoreactive complex. This step indeed requires synthesis and purification of the Ru-ODN conjugate. Thus, if photo-cross-linking of duplexes could be induced without preliminary synthetic steps for anchoring the Ru complex to the ODN, this would be very attractive and useful for biological applications including possible developments as photoprobes or photoreagents.<sup>7</sup>

It has been found that  $[\text{Ru}(\text{HAT})_2(\text{phen})]^{2+}$  (2; phen = 1,10-phenanthroline) illuminated in the presence of GMP produces not only an adduct of one G with one of the HAT ligands (Figure 2) but also a bis-adduct, corresponding to the addition of two guanine bases on the same complex.<sup>4</sup> This suggests that such a complex in interaction with a defined duplex containing a guanine moiety in close vicinity on each strand could give rise to a photo-cross-linking reaction. To confirm this hypothesis, we have chosen ODN duplexes **ds0–ds4** (ds = double strand) that contain one G on each strand, separated from each other by a variable number of base pairs (Table 1). Here, we focus not only on complex 2 but also on two other complexes containing two TAP ligands:  $[\text{Ru}(\text{TAP})_2(\text{phen})]^{2+}$  (1) and  $[\text{Ru}(\text{TAP})_2\text{TPAC}]^{2+}$  (3; TPAC = tetrapyridoacridine; Figure 1). Complexes 1–3 are indeed

**Table 1.** ODN Duplexes **ds0–ds4** and **Ru-ds**<sup>a</sup>

duplex	sequence	distance between G amino nitrogens (Å)	distance between G keto oxygens (Å)
<b>ds0</b>	5'-TTT TCG TTT TAA ATT TA-3' 3'-AAA AGC AAA ATT TAA AT-5'	3.9	3.9
<b>ds1</b>	5'-TTT TTT TCT GAA ATT TA-3' 3'-AAA AAA AGA CTT TAA AT-5'	7.6	7.2
<b>ds2</b>	5'-TTT TTT TCT AGA ATT TA-3' 3'-AAA AAA AGA TCT TAA AT-5'	11.3	10.4
<b>ds3</b>	5'-TTT TTT CTT AGA ATT TA-3' 3'-AAA AAA GAA TCT TAA AT-5'	14.8	13.7
<b>ds4</b>	5'-TTT TTC TTT AGA ATT TA-3' 3'-AAA AAG AAA TCT TAA AT-5'	18.1	16.9
<b>Ru-ds</b>	5'-TTT TTT CCX TAA ATT TA-3' 3'-AAA AAA GGA ATT TAA AT-5'		

<sup>a</sup> **Ru-ds** was used as a reference for the PAGE experiments (see further); its structure and photochemical and photophysical properties have been described previously.<sup>6</sup> X = thymidine modified with a linker bearing the Ru complex. The anchored Ru complex is  $[\text{Ru}(\text{TAP})_2(\text{dip})]^{2+}$  (dip = 4,7-diphenyl-1,10-phenanthroline).

expected to photo-cross-link the two strands, as they produce an adduct on a G base, while interacting with DNA in different ways.<sup>3,4,8</sup>

## Experimental Section

**Materials.** Complexes 1–3 were synthesized as previously described.<sup>1,3,4</sup> The different ODNs were prepared on an automated DNA synthesizer (ABI3400) by using the protocol described by the manufacturer and were purified by PAGE. The formation of the duplexes were performed by heating the <sup>32</sup>P-labeled ODN single strands (ss) with their complementary strands at 85 °C for 5 min and cooling slowly to room temperature for at least 6 h. Calf-thymus DNA (CT-DNA), dialyzed

(6) Lentzen, O.; Constant, J.-F.; Defrancq, E.; Prevost, M.; Schumm, S.; Moucheron, C.; Dumy, P.; Kirsch-De Mesmaeker, A. *ChemBioChem* **2003**, *4*, 195–202.

(7) Moucheron, C. *New J. Chem.* **2009**, *33*, 235–245 and references cited therein.

(8) Herman, L. Ph.D. thesis, Université libre de Bruxelles, Brussels, Belgium, November 2008.

several times against a buffer solution, was purchased from Sigma. Spectrophotometric-grade glycerol (99.5+%) was purchased from Janssen Chimica (Belgium) for the anisotropy measurements (see below).

**PAGE Experiments.** Before the analyses by gel electrophoresis, the illuminations of the complexes in the presence of the duplexes with the desired concentration ratios were carried out with a He/Cd laser remote controller, Omnichrome LC-500 (442 nm; power, 35 mW; intensity,  $36.8 \times 10^3 \text{ W m}^{-2}$ ; diameter of the beam, 1.1 mm; Melles Griot). A total of 100  $\mu\text{L}$  of solution was illuminated in an open Eppendorf placed horizontally in front of the beam. A total of 10  $\mu\text{L}$  of this illuminated solution was diluted with 10  $\mu\text{L}$  of buffer and deposited on the gel. The PAGE experiments under denaturing conditions were performed with 20% polyacrylamide (19:1 ratio of acrylamide to bisacrylamide), 7 M urea, and a TBE buffer (90 mM Tris-borate, pH = 8, and 2 mM EDTA). The labeled ODNs were visualized by autoradiography with a Storage Phosphor Screen (Amersham) film and a Phosphor-Imager Storm 860 instrument. The ODNs were 5'-labeled using polynucleotide kinase (Pharmacia Biotech) and [ $\gamma$ - $^{32}\text{P}$ ] ATP (Pharmacia Biotech) at 37 °C for 30 min.

**Emission Anisotropy.** Emission anisotropy data were obtained by the L-format method using an Edinburgh Instruments FS-900CDT steady-state spectrophotometer (Edinburgh Instruments, U. K.) equipped with a 450 W xenon lamp as the excitation source and a Peltier-cooled Hamamatsu R955 red-sensitive photomultiplier for detection. All measurements were temperature-controlled with a thermostatted circulating bath. The samples were excited at 450 nm, and the emission, measured through a Coherent-Ealing 495 nm cutoff filter, was collected between 500 and 800 nm with a constant bandwidth of 10.4 nm. Glan Thompson (calcite) polarizers were used for both the excitation and emission, and the anisotropy ( $r$ ) of the emitted light was calculated as previously described:<sup>9</sup>

$$r = \frac{I_{VV} - I_{VH(c)}}{I_{VV} + 2I_{VH(c)}} \quad (1)$$

where  $I_{IJ}$  represents the integration over the frequencies of the luminescence spectra recorded with different polarizations, the first subscript describing the excitation polarizer position (V<sub>ertical</sub> or H<sub>orizontal</sub>) and the second one the emission polarizer position.  $I_{VH(c)}$  is the integration of the corresponding emission spectrum corrected for the different sensitivities of the detection system for vertically and horizontally polarized light as

$$I_{VH(c)} = I_{VH} \frac{I_{HV}}{I_{HH}} \quad (2)$$

The samples consisted of 2.5  $\mu\text{M}$  ruthenium complex (**1–3**) in a 10 mM cacodylate buffer (pH 7.0)/glycerol mixture (50/50, v/v). When present, CT-DNA was used at a concentration of 187  $\mu\text{M}$  phosphate equivalents (phosphate/complex = 75) in order to ensure complete displacement of the binding equilibrium toward bound species. The circular dichroism (CD) spectrum of CT-DNA in the 10 mM cacodylate buffer (pH 7.0)/glycerol mixture (50/50, v/v) was recorded and showed the typical CD signature of B-form DNA (a positive band centered at 275 nm, a negative band at 240 nm, and the intersection with the abscissa axis at 259 nm).<sup>10</sup> This confirms that the secondary structure of CT-DNA is retained in the solvent mixture used for the anisotropy measurements.

**Molecular Modeling Simulations.** The structure of the Ru complexes **2–3** was obtained by DFT calculations with B3LYP/

6-31G (LANL2DZ for Ru), and constraints were imposed to maintain these optimized geometries for subsequent molecular mechanics simulations. The partial charges were recalculated with the Qeq method<sup>11</sup> after having imposed +2.0 charges on the ruthenium(II) centers, that is, giving a total charge of +2 for **2** and **3**. The ODNs were built from the Biopolymers module available in the Discovery Studio 2.0 package from Accelrys. The CHARMM force field<sup>12</sup> (v.22, modified version of 2006) was used, as it accurately describes nucleotides together with small organic molecules and has atom parameters for Ru atoms. For all of the simulations, the water solvent was implicitly taken into account via the use of the generalized Born model with a simple smoothing function.<sup>13</sup> Several geometries and distances between the complexes and DNA were tested (similarly to the docking approach), and the evolution of the total energy was followed as a function of the distance.<sup>14</sup> For energy minimization, the adopted basis Newton–Raphson algorithm was used with a rms distance of  $10^{-2} \text{ kcal/mol \AA}$ .

**Affinity Measurements.** The SPR measurements were performed on a BIAcore T100 (BIAcore AB, Sweden) operated with BIAcore T100 Evaluation Software 1.1. The experiments were carried out at 25 °C, using as a working buffer an aqueous solution of 10 mM HEPES at a pH of 7.4, 100 mM NaCl, 100 mM KCl, and 3 mM EDTA supplemented by 0.05% v/v P20 surfactant. The hairpin duplex d(5'-GCGCGCGCTTTTGCGCGCGC-3') was immobilized on a Streptavidin-coated surface (SA sensor chip, BIAcore AB) via a peptidic scaffold possessing a biotin residue.<sup>15</sup> This sequence was used as guanine-rich double-stranded DNA (ds-DNA). Binding experiments were conducted at 30  $\mu\text{L min}^{-1}$  by the injection of **3** dissolved in a buffer at concentrations from 50 to 1000 nM (injection time, 120 s; dissociation time, 500s). A non modified channel was used as a reference. Curves obtained from the reference surface were subtracted from the curves recorded after host–guest recognition, allowing elimination of refractive index changes (due to buffer effects) and corrections of the nonspecific interaction of **3** with the Streptavidin surface. These optimized experimental conditions allowed clear sensorgrams to be collected and interpreted in order to evaluate the affinity of **3** for ds-DNA (see the Supporting Information).

## Results and Discussion

**Emission Anisotropy and Affinity Measurements: Comparison with Molecular Modeling Calculations.** Before discussing the photo-cross-linking per se, it is important to know whether complexes **1–3** do interact with the duplex and, most importantly, have the possibility to move inside the duplex grooves during their excited state lifetimes in order to bridge the strands at the level of the G bases (either at the two amino or the two keto groups, Figure 2). The measurement of the emission anisotropy from the photoexcited <sup>3</sup>MLCT state, a spectroscopic technique furnishing information on the mobility of an excited luminescent species, should confirm/undermine this possibility. It is assumed that, if a loss of light emission polarization (originating from a fast motion of the excited molecule) occurs, the reduced complex formed

(11) Rappé, A. K.; Goddard, W. A., III. *J. Phys. Chem.* **1991**, *95*, 3358–3363.

(12) (a) Momany, F. A.; Rone, R. *J. Comput. Chem.* **1992**, *13*, 888. (b) MacKerell, A. D.; Banavali, N.; Foloppe, N. *Biopolymers* **2001**, *56*, 257–265.

(13) (a) Im, W.; Lee, M. S.; Brooks, C. L., III. *J. Comput. Chem.* **2003**, *24*, 1691–1702. (b) Im, W.; Feig, M.; Brooks, C. L., III. *Biophys. J.* **2003**, *85*, 2900–2918.

(14) Han, D.; Wang, H.; Ren, N. *THEOCHEM* **2004**, *711*, 185–192.

(15) Murat, P.; Cressend, D.; Spinelli, N.; Van der Heyden, A.; Labbé, P.; Dumy, P.; Defrancq, E. *ChemBioChem* **2008**, *9*, 2588–2591.

(9) Lakowicz, J. R. *Principles of Fluorescence Spectroscopy*, 2nd ed.; Kluwer Academic/Plenum: New York, 1999.

(10) Rodger, A.; Nordén, B. *Circular Dichroism and Linear Dichroism*; Oxford University Press: Oxford, U.K., 1997.

**Table 2.** Anisotropy ( $r$ ) Data in the Absence and in the Presence of CT-DNA<sup>a</sup>

complex	$r$	
	without CT-DNA	with CT-DNA
[Ru(TAP) <sub>2</sub> phen] <sup>2+</sup> ( <b>1</b> )	0.002	0.020
[Ru(HAT) <sub>2</sub> phen] <sup>2+</sup> ( <b>2</b> )	0.001	0.018
[Ru(TAP) <sub>2</sub> TPAC] <sup>2+</sup> ( <b>3</b> ) <sup>b</sup>	0.005	0.054
[Ru(bpy) <sub>2</sub> dppz] <sup>2+</sup> <sup>c</sup>		0.048
[Ru(bpy) <sub>3</sub> ] <sup>2+</sup> <sup>c</sup>	0.0007	0.004
[Ru(phen) <sub>3</sub> ] <sup>2+</sup> <sup>c</sup>	0.001	0.018

<sup>a</sup> Measurements were performed with complex concentrations of 2.5  $\mu$ M in a 10 mM cacodylate buffer (pH 7.0)/glycerol mixture (50:50, v/v) at +12 °C unless otherwise specified. The CT-DNA concentration was 187  $\mu$ M phosphate equivalents. The samples were excited at 450 nm, and the emission was collected between 500 and 800 nm. Error with CT-DNA = 8%. <sup>b</sup> This solution contained, in addition, 80 mM NaCl. <sup>c</sup> Anisotropy ( $r$ ) values calculated from the polarization ( $P$ ) values reported in the literature ([Ru] = 10  $\mu$ M, [DNA] = 1 mM in 20 mM sodium phosphate buffer (pH 7.85), 10 mM NaCl/glycerol 40:60).<sup>16</sup> bpy = 2,2'-bipyridine; dppz = dipyrido[3,2-*a*:2',3'-*c*]phenazine.

from the excited molecule after the ET reaction can also move or rotate inside the DNA duplex. Whereas the light emission polarization gives indication of the excited complex, it is indeed the reduced complex which has to react with the oxidized G unit generated after the photo-induced ET to give rise to the adduct.

The anisotropy ( $r$ ) of the <sup>3</sup>MLCT emission of the three complexes **1–3** was measured in the absence and in the presence of CT-DNA in a buffer/glycerol mixture in order to assess the importance of a possible immobilization of these complexes upon DNA binding. The values of  $r$  under the steady state conditions are collected in Table 2, together with values reported in the literature for other Ru(II) complexes interacting with DNA by different binding modes. Whereas the emission of **1–3** is almost completely depolarized in a buffer solution containing 50% glycerol, a significant retention of anisotropy is observed in the presence of CT-DNA for each complex.

**i.** [Ru(TAP)<sub>2</sub>TPAC]<sup>2+</sup> (**3**). Complex **3** displays the largest emission anisotropy ( $r$ ) upon DNA binding, with an  $r$  value similar to that reported for the metallo-intercalator [Ru(bpy)<sub>2</sub>dppz]<sup>2+</sup> (bpy = 2,2'-bipyridine; dppz = dipyrido[3,2-*a*:2',3'-*c*]phenazine).<sup>16</sup> Therefore, it is also proposed that this higher  $r$  value for **3** stems from the intercalation of its extended planar ligand TPAC within the base pairs stack of DNA. The previously demonstrated DNA intercalation of several complexes such as [Ru(L)<sub>2</sub>dppz]<sup>2+</sup> (where L = bpy, phen, and TAP),<sup>2,17–19</sup> [Ru(L)<sub>2</sub>PHEHAT]<sup>2+</sup> (PHEHAT = 1,10-phenanthroline-[5,6-*b*]-1,4,5,8,9,12-hexaazatriphenylene, with L = phen or TAP),<sup>20,21</sup> or [Ru(bpy)<sub>2</sub>tpphz]<sup>2+</sup> (tpphz = tetrapyrido-[3,2-*a*:2',3'-*c*:3'',2''-*h*:2''',3'''-*j*]-phenazine),<sup>22</sup> which are

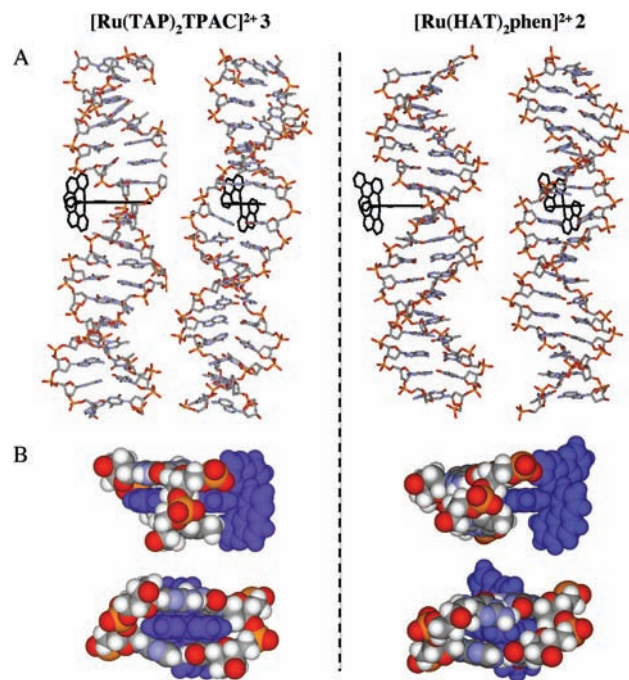


**Figure 3.** (A) “Stick” views of molecular modeling simulations of the intercalation of **3** (left) and **2** (right) into **ds4**. Hydrogen atoms are not shown for the sake of clarity. (B) “Corey–Pauling–Koltun” views of molecular modeling simulations of the intercalation of **3** (left) and **2** (right) into **ds4**. Only the adjacent bases are depicted.

structurally related to TPAC, affords further support to the proposed intercalative binding mode of **3**. This complex exhibits also a high binding affinity for DNA ( $1.5 \times 10^6$  M<sup>-1</sup> as measured from SPR experiments in the presence of 100 mM NaCl and 100 mM KCl, see the Supporting Information).

Molecular mechanics simulations of **3** bound to the double-stranded 17-mer **ds4** were performed using the docking methodology. The results of these molecular modeling calculations are also consistent with the intercalation of **3** within the regular B-type double helix structure of this 17-mer. The 9.1 Å distance between two H atoms along the TPAC short axis is small enough to allow its insertion within the base pairs stack of the ODN in which the two complementary strands are separated by a distance of 10.9 Å, calculated between the two carbon atoms of the opposite ribose moieties belonging to the complementary H-bonded bases. Figure 3A,B shows a minimum energy conformation with the TPAC planar aromatic ligand stacked between the G–C and T–A base pair planes of **ds4** in the major groove. The intercalation of **3** induces a slight increase of the minor groove width of the ODN duplex (about 3 Å) together with a lengthening of the helix (about 3.6 Å). In addition, a flipping of the bases, often referred to as propeller twist, buckle, and tilt in the coordinate frame of DNA, occurs at the intercalation site and also, to a smaller degree, largely beyond the immediate vicinity of the intercalation pocket. This long-range flipping of the bases, typical of intercalation, promotes the formation of multiple H bonds between adjacent base pairs whose number increases from 36 H bonds in **ds4** to 41. Such conformational changes have already been shown to occur upon DNA binding of metallo-intercalators from high-resolution X-ray

(16) Delaney, S.; Pascaly, M.; Bhattacharya, P. K.; Han, K.; Barton, J. K. *Inorg. Chem.* **2002**, *41*, 1966–1974.

(17) Lincoln, P.; Nordén, B. *J. Phys. Chem. B* **1998**, *102*, 9583–9594.

(18) Zeglis, B. M.; Pierre, V. C.; Barton, J. K. *Chem. Commun.* **2007**, 4565–4579 and references therein.

(19) Ortman, I.; Elias, B.; Kelly, J. M.; Moucheron, C.; Kirsch-De Mesmaeker, A. *Dalton Trans.* **2004**, 668–676.

(20) Moucheron, C.; Kirsch-De Mesmaeker, A.; Choua, S. *Inorg. Chem.* **1997**, *36*, 584–592.

(21) Moucheron, C.; Kirsch-De Mesmaeker, A. *J. Phys. Org. Chem.* **1998**, *11*, 577–583.

(22) Liu, Y.; Chouai, A.; Degtyareva, N.; Lutterman, D. A.; Dunbar, K. R.; Turro, C. *J. Am. Chem. Soc.* **2005**, *127*, 10796–10797.

structure determination.<sup>23</sup> At the intercalation site (as shown in Figure 3A,B), the TPAC is deeply inserted in the base pairs stack of the double helical ODN. Although a complete insertion of the TPAC ligand remains excluded because of the steric constraints between the ancillary TAP ligands and the DNA backbone, more than half of its aromatic surface is actually involved in stacking interactions with the nucleobases. This suggests, in agreement with the anisotropy measurements, that the mobility of **3** should be restricted within the duplex intercalation pocket. The effect of these geometrical constraints on the possible photo-cross-linking of the different 17-mers by complex **3** is discussed in the next section.

ii.  $[\text{Ru}(\text{HAT})_2\text{phen}]^{2+}$  (**2**). The DNA binding of complex **2** was previously studied, and a weak affinity constant of  $5.0 \times 10^3 \text{ M}^{-1}$  was obtained with 50 mM NaCl.<sup>4,24</sup> The substantial contribution of the nonelectrostatic interactions to the binding free energy and the slight increase of DNA viscosity upon the addition of **2**,<sup>4</sup> albeit smaller than with a classical intercalator such as ethidium bromide, led to the conclusion that one HAT ligand should be partially intercalated within the stacking of DNA bases. In agreement with this conclusion, the retention of emission polarization anisotropy of **2** in the presence of DNA is significantly lower than that for a classical metallo-intercalator. Molecular modeling calculations confirm these observations and show that, in contrast to **3**, the extended aromatic HAT ligand is only slightly intercalated, with almost no  $\pi$ -stacking interactions between the HAT plane and the neighboring DNA base pairs (Figure 3A,B). The presence of the second HAT ligand, which is much more hindering as compared to the TAP ancillary ligands of **3**, gives rise to a strong steric crowding with the duplex backbone and prevents a deep insertion of the semi-intercalated HAT ligand of **2** in the base pairs stack. Whereas a lengthening of the duplex of about 3.6 Å typical of a  $\pi$ -stacking distance was calculated for the intercalation of **3**, the duplex length only increases by 2.8 Å upon the binding of **2**, affording further support for a *semi*- or *quasi*-intercalative binding mode for **2**. The main conclusion that may be drawn from the anisotropy measurements and molecular mechanics simulations is thus that the reorientation or mobility of **2** bound to DNA by *semi*- or *quasi*-intercalation is not as largely restricted as for classical metallo-intercalators.

iii.  $[\text{Ru}(\text{TAP})_2\text{phen}]^{2+}$  (**1**). The binding affinity of **1** to DNA ( $K = 3.9 \times 10^4 \text{ M}^{-1}$  in a buffer in the absence of added NaCl) has been reported previously, and it was shown that **1** exhibits a nonintercalative binding mode with DNA.<sup>24,25</sup> The emission of **1** bound to DNA is polarized to a similar extent as that of **2** or its homoleptic phenanthroline geometrical analogue  $[\text{Ru}(\text{phen})_3]^{2+}$ , which does not intercalate either.

**Photo-Cross-Linking Study.** The photo-cross-linking was studied by polyacrylamide gel electrophoresis

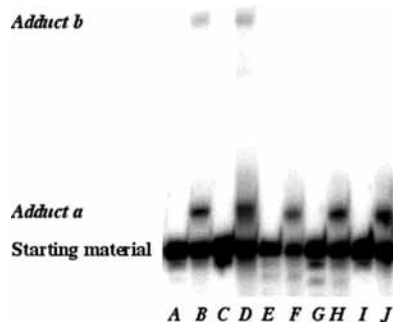


**Figure 4.** Denaturing gel electrophoresis of 17-mers ODN **ds0**–**ds4** (80  $\mu\text{M}$ ) in the presence of  $[\text{Ru}(\text{TAP})_2\text{phen}]^{2+}$  (**1**; 80  $\mu\text{M}$ ) in 80 mM NaCl and 10 mM Tris HCl buffer at pH = 7. Lane A, **ds0**; lane B, **ds0** after 30 min illumination; lane C, **ds1**; lane D, **ds1** after 30 min illumination; lane E, **ds2**; lane F, **ds2** after 30 min illumination; lane G, **ds3**; lane H, **ds3** after 30 min illumination; lane I, **ds4**; lane J, **ds4** after 30 min illumination.

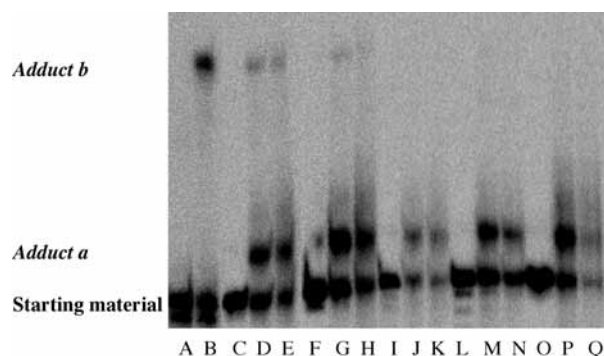


**Figure 5.** Denaturing gel electrophoresis of 17-mer ODN **ds0**–**ds4** (80  $\mu\text{M}$ ) in the presence of  $[\text{Ru}(\text{HAT})_2\text{phen}]^{2+}$  (**2**; 80  $\mu\text{M}$ ) in 50 mM NaCl and 10 mM Tris HCl buffer at a pH of 7. Lane A, **Ru-ds**; lane B, **Ru-ds** after 30 min illumination; lane C, **ds0**; lane D, **ds0** after 30 min illumination; lane E, **ds0** after 60 min illumination; lane F, **ds1**; lane G, **ds1** after 30 min illumination; lane H, **ds1** after 60 min illumination; lane I, **ds2**; lane J, **ds2** after 30 min illumination; lane K, **ds2** after 60 min illumination; lane L, **ds3**; lane M, **ds3** after 30 min illumination; lane N, **ds3** after 60 min illumination; lane O, **ds4**; lane P, **ds4** plus 30 min illumination; lane Q, **ds4** after 60 min illumination.

(PAGE) experiments under denaturing conditions (Figures 4–6). If the 5' end of one of the strands of the duplex is <sup>32</sup>P-labeled and if a photo-cross-linking occurs between the two strands, a spot migrating as a duplex, thus a retarded band, has to be visualized on the gel by radioactive counting, even under denaturing conditions as the two strands are then linked by covalent bonds. In contrast, if no photo-cross-linking takes place, only bands migrating as single strands have to be observed in these conditions. In order to determine the electrophoretic mobility of a covalently linked duplex under the conditions used for these experiments, a reference duplex **Ru-ds** was also deposited on the gels. This reference consisted of an irradiated duplex with the same length as sequences **ds0**–**ds4** and was composed of a strand chemically derivatized by the photoactivable  $[\text{Ru}(\text{TAP})_2\text{dip}]^{2+}$  (**dip** = 4,7-diphenylphenanthroline) complex and the complementary sequence containing two guanine moieties in close vicinity of the attached complex (see Table 1 for the sequence). It was shown that the illumination in the visible of such a **Ru-ds** leads to an irreversible photo-cross-linking of the two strands (compare lanes A before illumination and B after

(23) Kielkopf, C. L.; Erkkila, K. E.; Hudson, B. P.; Barton, J. K.; Rees, D. *C. Nat. Struct. Biol.* **2000**, *7*, 117–121.

(24) The binding affinity of complexes **1** and **2** for CT-DNA was previously measured by titration of the complex emission as a function of increasing DNA concentrations (in equivalent phosphate) at constant complex concentration. It should be noted that these values are too small to perform surface plasmon resonance measurements like for **3**.

(25) Del Guerzo, A.; Kirsch-De Mesmaeker, A. *Inorg. Chem.* **2002**, *41*, 938–945.

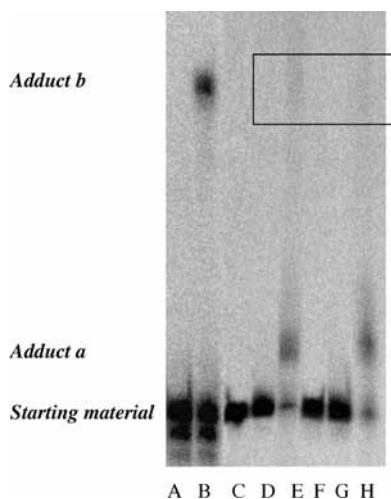


**Figure 6.** Denaturing gel electrophoresis of 17-mer ODN (60  $\mu\text{M}$ ) in the presence of  $[\text{Ru}(\text{TAP})_2\text{TPAC}]^{2+}$  (**3**; 60  $\mu\text{M}$ ) in 80 mM NaCl, [base pair]/[Ru] = 1. Lane A, **Ru-ds**; lane B, **Ru-ds** after 30 min illumination; lane C, **ds0** in absence of **3**; lane D, **ds0** in presence of **3**; lane E, **ds0** after 30 min illumination; lane F, **ds1** in absence of **3**; lane G, **ds1** in presence of **3**; lane H, **ds1** after 30 min illumination.

illumination, in Figures 5 and 6), and the isolated spots after illumination, analyzed by mass spectrometry, confirmed the presence of covalent bond formation between the complex and the ODN.<sup>1,5,6</sup>

Both complexes **1** and **2** show a similar behavior in the presence of the different duplexes; thus photoproducts noted as adducts **a** and **b** are detected (shown in Figure 4 for complex **1** and in Figure 5 for complex **2**). Adduct **b** has the same electrophoretic mobility as the reference duplex **Ru-ds** after illumination (Figure 5). Therefore, adduct **b** corresponds to a photo-cross-linking reaction between the two strands. Adduct **a**, which migrates slightly less than the single strand, corresponds to the monoadduct of the complex on the G base of the <sup>32</sup>P-labeled single strand. This type of adduct was analyzed previously by mass spectrometry.<sup>4</sup> Although adduct **a** appears after illumination of complexes **1** and **2** in the presence of each ds-ODN, adduct **b** in contrast is detected only for the ODNs in which there is 0 or 1 base pair between the two G bases (lanes B and D in Figure 4 and lanes D and E and lanes G and H in Figure 5). It is difficult to conclude which double-stranded ODNs (**ds0** or **ds1**) lead to the higher photo-cross-linking because the differences in percentages are not sufficient. It has to be noted that the ratio “[base pair]/[complex]” corresponds to 1:1 for each experiment. Consequently, taking into account the low affinity constant of complexes **1** and **2** for DNA, that is,  $3.9 \times 10^4 \text{ M}^{-1}$  and  $2.4 \times 10^5 \text{ M}^{-1}$ , respectively, in a buffer in the absence of added NaCl,<sup>4,25</sup> and considering the rather high NaCl concentration under the present conditions, only a small fraction of the complexes should be bound to the duplexes. With these weak affinities, the adduct **b** corresponding to the photo-cross-linking reaches, for **ds0** or **ds1**, 2–3% for  $[\text{Ru}(\text{TAP})_2(\text{phen})]^{2+}$  (**1**) and 5–6% (**ds0**) or 2% (**ds1**) for  $[\text{Ru}(\text{HAT})_2(\text{phen})]^{2+}$  (**2**) after 30 min of illumination.

Table 3 gives for complex **2** and **ds0** the percentages in intensity of the bands corresponding to both photo-adducts **a** and **b** as a function of the illumination time. The percentage of adduct **a** reaches 40% during the first

**Table 3.** Percentages of Photoadducts **a** and **b** (i.e., photo-cross-linking) for  $[\text{Ru}(\text{HAT})_2(\text{phen})]^{2+}$  (**2**) with **ds0** in the Presence of 80 mM NaCl for Different Illumination Times, [base pair]/[Ru] = 1

[Ru(HAT) <sub>2</sub> (phen)]Cl <sub>2</sub>			
time (min)	% remaining ODN	% adduct <b>a</b>	% adduct <b>b</b>
30	56	39	5
60	47	47	6
90	52	41	7
120	50	41	9

15 min of illumination (result not shown); afterward, the intensity of this band increases more slowly and even starts decreasing. In parallel, the percentage of intensity of the band corresponding to the photo-cross-linking (adduct **b**) increases slowly up to ~10%. This behavior indicates that a sufficient amount of adduct **a** has first to be formed (40%) before detecting clearly the band corresponding to the photo-cross-linked duplex (adduct **b**). Thus, enough adduct **a** has to accumulate to absorb enough light to give rise to the two G adducts and, thus, in this way bridge the two G bases belonging to the two complementary strands. Therefore, the yield cannot be very high as the photo-cross-linking originates from the successive absorption of two photons. This observation is also in agreement with the low yield of formation of products corresponding to the addition of two G units on the same complex, as evidenced previously with  $[\text{Ru}(\text{HAT})_2(\text{phen})]^{2+}$  illuminated in the presence of GMP.<sup>4</sup>

It should be noted that the percentage of starting ODN remains fairly constant after a certain illumination time. This observation has already been described in the literature<sup>26</sup> and could be due to a more important absorption of light by the monoadduct than by the initial complex and to some photodechelation of the Ru complex which consumes the initial photoreagent.

For complex **3**, which does intercalate and has a high affinity for DNA, the use of a ratio [base pair]/[Ru] = 80  $\mu\text{M}$ /80  $\mu\text{M}$  = 1:1 as with complexes **1** and **2** does not allow a direct comparison with the results obtained with those two compounds. Under such conditions, the duplex would be overloaded by complex **3** so that, in addition to intercalated Ru species, adsorbed Ru complex on the DNA double strands would also be present. Therefore, a ratio [base pair]/[Ru] = 55  $\mu\text{M}$ /15  $\mu\text{M}$  = 3.6:1 has been used to perform the gel experiments under the same conditions of loading as those used for complexes **1** and **2**. Under those conditions of identical loading level of the duplex by complex **3**, the bands corresponding to the photo-cross-linking cannot be detected after 30 min of illumination (see the Supporting Information).

By using the same ratio “[base pair]/[complex] = 1:1”, as with complexes **1** and **2**, overloading thereby the double-stranded ODN with complex **3**, the photo-cross-linking can be barely detected (Figure 6). Although 10% photo-cross-linking is given in Table 4 after 30 min of illumination, this value should be considered as overestimated because a certain amount of ODN has been decomposed

(26) Vicendo, P.; Mouysset, S.; Paillous, N. *Photochem. Photobiol.* **1997**, *65*, 647–655. Uji-i, H.; Foubert, P.; De Schryver, F. C.; De Feyter, S.; Gicquel, E.; Etoc, A.; Moucheron, C.; Kirsch-De Mesmaeker, A. *Chem. Eur. J.* **2006**, *12*, 758–762.

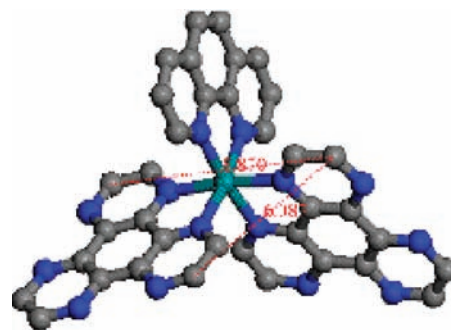
**Table 4.** Percentages of Photoadducts **a** and **b** for  $[\text{Ru}(\text{TAP})_2\text{TPAC}]^{2+}$  (**3**) with Duplexes **ds0** and **ds1** in the Presence of 80 mM NaCl [base pair]/[Ru] = 1:1

oligonucleotides	time (min)	% remaining ODN	% adduct <b>a</b>	% adduct <b>b</b>
<b>ds0</b>	30	38	52	10
<b>ds1</b>	30	34	60	6

under such conditions after illumination in the presence of complex **3**. Moreover, the smears that accompany each band, caused by the adsorption of **3** on the ODN (ss or ds) make quantitative determinations rather difficult.<sup>27</sup>

In spite of these problems, some interesting conclusions can be drawn from the behavior of  $[\text{Ru}(\text{TAP})_2\text{TPAC}]^{2+}$  complex **3**. When the ODN is not or is less overloaded by complex **3**, thus when the intercalation binding mode predominates, no photo-cross-linking is observable (see the Supporting Information). This could be attributed to the intercalation of the Ru TPAC complex, which induces a poor mobility inside the ODN double helix and consequently hinders the access to the nitrogen (or oxygen) groups of the G bases on each strand. In contrast, under conditions in which the ODN is overloaded by the complex, thus when complex **3** binds to DNA not only by intercalation but also by adsorption (Figure 6), photo-cross-linking occurs (10% after 30 min probably overestimated, Table 4).<sup>28</sup>

Considering again the cases of  $[\text{Ru}(\text{TAP})_2(\text{phen})]^{2+}$  (**1**) and  $[\text{Ru}(\text{HAT})_2\text{phen}]^{2+}$  (**2**), for which bands corresponding to photo-cross-linking can clearly be detected (Figures 4 and 5), photo-cross-linking is observed only when 0 or 1 base pair between the G bases is present. For the different sequences that have been tested, the distances between the two nitrogens of the two G's amino groups (or between the two oxygens of these two G's keto groups) have been calculated from molecular modeling (columns 3 and 4 in Table 1). This distance is 3.9 Å and 7.6 Å (or 7.2 Å) for **ds0** and **ds1**, respectively. If we compare these distances to those between two carbons in the  $\alpha$  position of the nitrogens of the TAP ligand, either belonging to the two TAPs (or two HATs, 8.7 Å) or to the same TAP (or same HAT, 6.1 Å; see Figure 7), which correspond to the positions where covalent bonds between the Ru complex and the G units should be formed,<sup>4,5</sup> we reach the following conclusion. These distances in Figure 7 are larger than those between the two G bases of **ds0** (3.9 Å) but compatible with those of **ds1** (7.6 or 7.2 Å). This implies, as both complexes photo-cross-link **ds0** and **ds1** without significant differences in percentages, that distortion of the double helix takes place during the photo-reaction, at least for **ds0**. It is indeed expected that the formation of the first covalent bond with the G perturbs H-bondings in the duplex, which distorts the ODN. For **ds2** and the other tested ODNs (Table 1) the G–G distances are larger than the above considered carbon–carbon distances of complexes **1** and **2** so that the distortion of the ODN

**Figure 7.** Two possible C–C distances, that is, inter- and intraligand, for complex  $[\text{Ru}(\text{HAT})_2\text{phen}]^{2+}$  (**2**). The distances are the same for complex **1**. These carbon atoms correspond to the reactive positions (see Figure 2A,B) giving rise to the adduct. The hydrogen atoms are omitted for clarity.

should become too large for a photo-cross-linking to take place, which is in agreement with the results. From these considerations, it seems reasonable that high mobility or an appropriate geometry of the system is required for the photo-cross-linking. Such a flexibility is not compatible with the intercalation geometry of **3** but is consistent with the higher mobility of complexes **1** and **2**, as shown by the low retention of emission polarization.

## Conclusion

As mentioned in the Introduction, we had observed by mass spectrometry in a previous study that two GMP molecules can be added covalently on one complex, **2**, under illumination.<sup>4</sup> In this study, we have demonstrated that **2** containing two HAT ligands and also complex **1** containing two TAP ligands are able to photo-cross-link two complementary ODN strands each comprising a G base, in close vicinity. The present data show also that, although complexes **1–3** respond to the conditions of photoreactivity, they exhibit a different behavior depending on their interaction geometry with the ODN duplexes. As **3** intercalates its TPAC ligand into the base pairs stack, its mobility is restricted in the duplex. Thus, higher levels of loading of DNA are required to saturate the DNA and observe photo-cross-linking. Consequently, intercalation, which could seem a better binding geometry to induce photo-cross-linking due to the high binding affinity, is not the most favorable interaction geometry to induce such photodamaging. These results provide therefore the guidelines needed for the development of interesting photoprobes and photoreagents of the genetic material.

**Acknowledgment.** The authors thank the Belgian Federal Science Policy (program IAP, P6/27) and the FRFC-FNRS (Belgian National Science Foundation) for financial support. They are also grateful to Leslie Herman and Igor Avilov for having provided the DFT-optimized geometric structures of the complexes. They thank COST for supporting the collaboration between the Belgian (ULB) and French teams. They are grateful to the NanoBio program for the facilities of the Synthesis and Surface Characterization platforms. F.P. and M.S. are postdoctoral researchers and D.B. a Research Director of the FNRS.

**Supporting Information Available:** Surface plasmon resonance (SPR) study and gel electrophoresis analysis. This material is available free of charge via the Internet at <http://pubs.acs.org>.

(27) We observed that such smears accompanying the spots on the gel are also present for a complex which is not photoreactive but contains also one TPAC ligand, that is, for  $[\text{Ru}(\text{phen})_2(\text{TPAC})]^{2+}$ .

(28) This overloading also induces other photoreactions such as ODN photocleavages into very small fragments whose radioactivity has not been recorded in the analyzed gels. This is in agreement with the very weak intensity of the radioactivity for the bands corresponding to the starting material, adduct **a**, and photo-cross-linking (Figure 6 and Supporting Information).